*Received: April 18, 2019*
*Revised: June 19, 2019*
*Accepted: June 25,2019*



# Vertically aligned ZnO nano-rods and its photo-conductive characteristics related to the catalytic properties

Suchada Worasawat[1,2 *], Katsuyoshi Tasaki[2], Yoichiro Neo[2], Yoshinori Hatanaka[2] and Hidenori Mimura[2 *]

*[1] Graduate school of science and technology and [2] Research Institute of Electronics, Shizuoka University, 3-5-1 Johoku, Naka-ku, Hamamatsu,432-8011, Japan*

## Abstract

Highly oriented and columnar crystalline zinc oxide (ZnO) nano-rods (NRs) were fabricated using two steps processes, consisting of seeding layer process by the RF magnetron sputtering and nano-rod growth process by the hydrothermal crystal growth. Samples as-grown were annealed in air at 250 and 450 ºC and characterized on the crystallinity and the photo-electrical properties. The ZnO NRs observed by FE-SEM showed a hexagonal column for the as-grown and annealed ZnO NRs samples. The XRD patterns showed wurtzite crystal structure perfectly oriented along with the c-axis (0002) direction and, by the annealing, supported to pushed up the development of ZnO NRs crystallinity. The photo-luminescence spectrum also showed an increase of band edge emission and a decrease of broad emission from crystal defect states with respect to the annealing process. The lowering of resistivity and outstanding of photo-conductivity were obtained from annealed ZnO NRs at 450ºC. Moreover, it was shown in the reaction with the environmental oxygen that the decay response of photo-excited carriers was accelerated by the assistance of oxygen molecules. These photo-conductivity measurements could be leading to investigate the photo-catalytic phenomenon on the surface of ZnO NRs.

**Keywords:** ZnO thin film, ZnO nano-rods, Hydrothermal crystal growth, Catalytic properties Photoconductivity

## 1. Introduction

Zinc oxide (ZnO) as a typical direct wide band gap semiconductor has extensively studied on the photo-electrical properties, having highly thermal and chemical stability at room temperature [1]. The photo-electrical properties of ZnO are affected by many factors, such as the structure [2] [3], size [4], shape [5][6], and defect concentration [7], which makes ZnO a very interesting application to develop novel devices. One dimensional (1D) ZnO such as nano-wire, nano-tubes and nano-rods have attracted attention in recent years due to their unique properties on the charge carrier transportation [8][9]. They are also expected to apply interconnects and functional units in electrochemical and photo-electrochemical applications [10] . 1D ZnO nano-structure has high surface to volume ratio and hence, it is suitable to employed in the photo-chemical application devices, such as UV detector, chemical sensor and gas sensor [11][12]. Chemical/gas sensitivity was strongly controlled by the oxygen-vacancy-related defect on the surface of the 1D ZnO nanostructure [13]. The electron trapping and recombination at the surface states strongly affect the photoconductivity. There are many research group studying the photoconductivity property of 1D ZnO nanostructure [14][15], Modifications of ZnO NRs with annealing process were reported showing higher photoconductivity than as-grown samples, due to the reduction of surface additives and surface defects in the ZnO NRs. However, there are little reports on catalytic reactions for the

*Corresponding Author E-mail: swoswat@gmail.com*

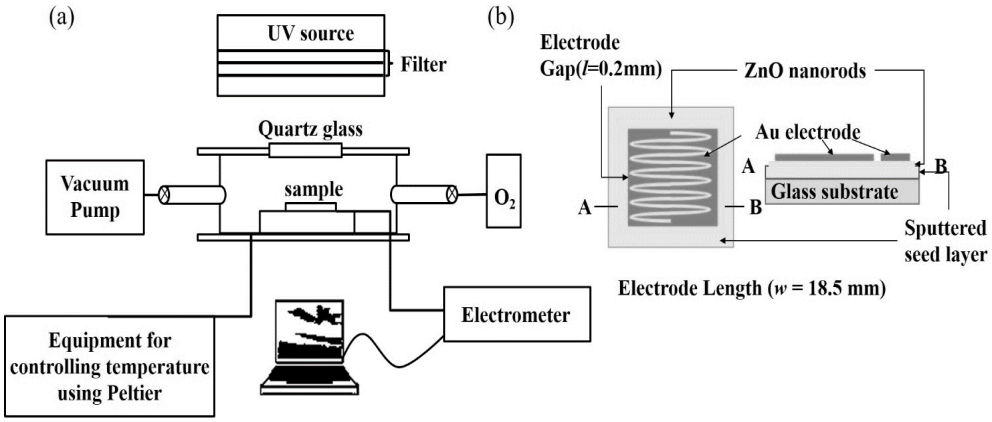


**Fig. 1.** The schematic diagram of (a) photoconductivity measurement system and (b) top-view and cross-section of sample with gold planar electrode.

surface of ZnO NRs in atmosphere. Hence, in this work we report the photoconductive phenomena of ZnO NRs films for explaining catalytic reaction under UV irradiation. Photo-catalytic are related to the reaction between electrons-holes and atmospheric molecules such as oxygen, hydrogen, and water at the surface [16-19].

Various processes have been developed to growth 1D ZnO nano-structure such as thermal evaporation, pulsed laser deposition, sol-gel method and hydrothermal process [20-24]. Among the methods, the hydrothermal process is favorable due to the low temperature process, large area growth, non-expensive and easy-controllable processes [25]. Moreover, the heat treatment processes are very easy for the sample by the hydrothermal growth to be modified the defect states of ZnO nano-structure [26]. Thus, the preparations and characterization of ZnO NRs array crystal including the annealing process and photo-conductivity measurements are described with the analytical consideration.

## 2. Experimental details

The growth of ZnO nano-structure was followed in the two-step processes: firstly, a seed layer was deposited on the glass substrates (Tempax, boron silicate glass) using RF sputtering technique. The sputtering was carried out using sintered ZnO disc target at the substrate temperature of 250°C, argon atmosphere 5 x$10^{-2}$ Pascal and RF power 100 W. Secondly, ZnO NRs crystals were grown by hydrothermal processes, the sample with the seed layer was transferred to the autoclave vessel. Zinc nitrate hexahydrate ($Zn(NO_3)_2$, Kanto Chemical Co., Inc.) and hexamethylenetetramine ($C_6H_{12}N_4$, Kanto Chemical Co., Inc.) 0.02 M were dissolved in de-ionized (DI) water 50 ml and transferred to the Teflon-lined autoclave. The sample with seed layer in the autoclave vessel was maintained at 60 ºC for 6 h. After the growth, the sample was washed by DI water and annealed at 100 ºC in air for 1 h. These samples were considered as as-grown ones. Moreover, some of the samples were further annealed at 250 and 450 ºC and compared to the as-grown sample on the properties of the photo-conduction, referring to the crystalline structure and optical properties. A surface morphology and the density-in-number of micro-crystals were examined by means of field emission scanning electron microscopy (FE-SEM; JEOL, JSM-7600F). The X-ray diffraction equipment (XRD; Rigaku – RINT - 2200, CuK radiation) was used to characterize a crystal

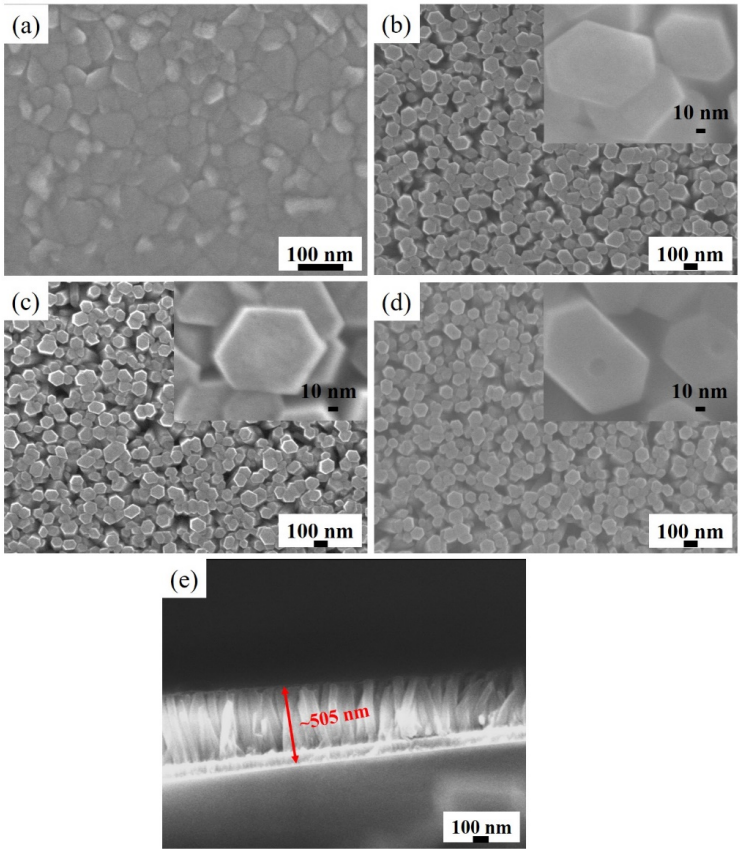


**Fig. 2.** The FE-SEM images of (a) sputtered seed layer, (b) as-grown, (c) annealed at 250ºC, (d) annealed at 450ºC, and (e) the cross-session of ZnO NRs annealed 450ºC.

structure of the grown ZnO nano-rods. The optical and electrical properties were investigated by the Photo-luminescent measurement (PL; IK Series He-Cd LASER) and photo-conductivity measurement which is consisted of vacuum chamber with UV window and inlet of oxygen and argon gas, in which the sample stage temperature is controlled by peltier element as shown in Fig. 1(a). The coplanar gold electrodes were deposited on the sample as shown in the Fig. 1(b).

## 3. Results and discussion

### 3.1 The structural and morphology properties of ZnO thin film

The FE-SEM images for the as-grown and annealed ZnO NRs thin films at 250 and 450ºC are shown in Fig. 2. From the images, well-oriented, hexagonal-shape ZnO NRs were observed with good uniformity and a high density of nanorods. The ZnO NRs are vertically grown to the substrate as shows in Fig. 2(e). The porous were observed on the nano-rods surface after annealed at 250 ºC and transferred to nano-holes after annealed at 450 ºC as shown in Fig. 2(c) and 2(d). It could be suspected that these porous and nano-holes are considered to result from the evaporation of weak bonding in the crystal, such as OH, NHx

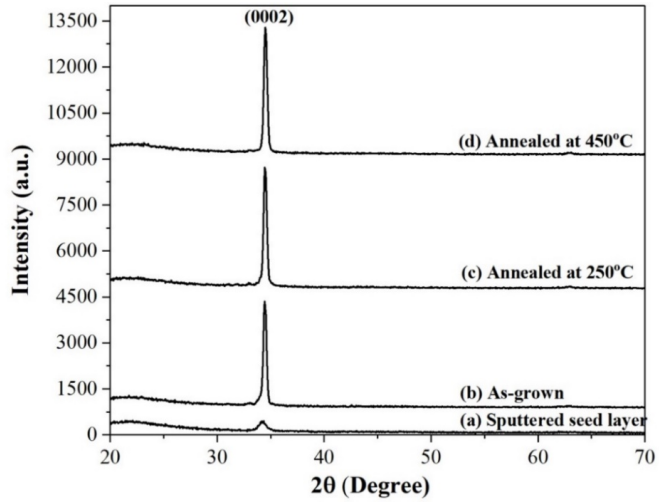


**Fig. 3.** The XRD pattern of sputtered seed layer and grown ZnO NRs film.

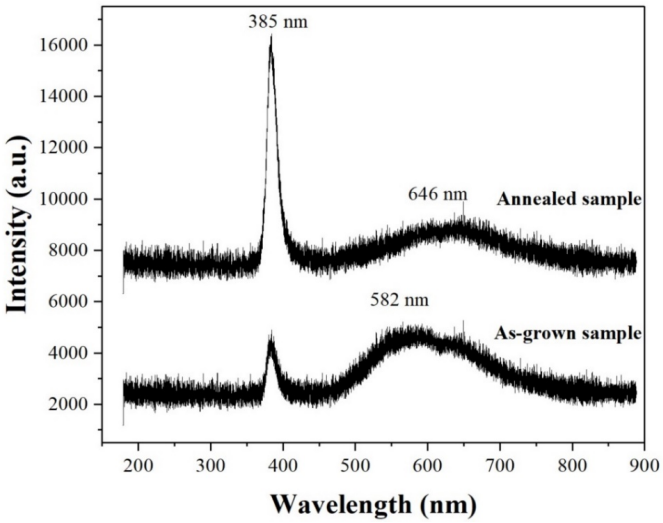


**Fig. 4.** The PL spectrum of ZnO NRs: as-grown and annealed sample.

and others, when annealed at high temperature [27]. Products of the chemical reaction between hexamethylenetetramine ($(CH_2)_6N_4$, or HTMA) and $Zn(NO_3)_2$ in hydrothermal solution are remained in or on the interstitial or surface as described the following: [28];

$$(CH_2)_6N_4 + 6H_2O \rightarrow 6HCHO + 4NH_3 \quad (1)$$

$$NH_3 + H_2O \leftrightarrow NH_4^+ + OH^- \quad (2)$$

$$2OH^- + Zn^{2+} \rightarrow Zn(OH)_2 \quad (3)$$

$$Zn(OH)_2 \rightarrow ZnO + H_2O \quad (4)$$

**Table 1.** The calculated values of crystalline size, resistivity, activation energy, decay life time, and dispersion parameter of ZnO NRs.

| Samples | Crystallite size (nm) | Resistivity (Ω·m) | Saturated current values (A) | Decay time (τ, min) | β |
|---|---|---|---|---|---|
| As-grown | 25 | $7.802 \times 10^{2}$ | $5.58 \times 10^{-5}$ | 100 | 0.78 |
| Annealed 250 ºC | 24 | $3.987 \times 10^{2}$ | $5.20 \times 10^{-5}$ | 63 | 0.87 |
| Annealed 450 ºC | 24 | $0.13 \times 10^{2}$ | $6.91 \times 10^{-4}$ | 17 | 0.78 |

Corresponding to the chemical reaction beyond the ZnO NRs growth, there are many additional products such as $NH_3$ and $OH^-$. Those products might be absorbed on the surface of ZnO NRs. Upon annealing at the high temperature, they may be evaporated from the surface of ZnO NRs.

Figure 3 shows XRD pattern of sputtered seeding layer, as-grown NRs and annealed NRs at 250ºC and 450 ºC on the glass substrate. All diffraction peaks were assigned (0002) plane according to the ZnO wurtzite structure (JCPDS No. 36-1451), indicating that the preferential growth of the nano-rods is along the c-axis. The (0002) peak of the annealed nano-rods was fairly two times higher than the as-grown ones. These results indicated that the crystallization is improved by the annealing process. The crystallite size of ZnO NRs is obtained by using Scherrer formula as in following;

$$D = \frac{0.9\lambda}{A\cos\theta} \tag{5}$$

Where D is crystallite size (nm), λ is the wavelength of X-ray (0.154 nm), A is the full width at half maximum (FWHM) of diffraction peak, and θ is the Bragg diffraction angle in degree. The data obtained are shown as about 25 nm in Table 1.

The photoluminescent spectrum (PL) was observed in room temperature shown in Fig. 4. The PL spectra shows two emission peaks; a sharp band edge emission at 385 nm and a broad defect band emission at 582 nm for the as-grown sample and at 646 nm for the annealed sample. After annealing process, it seems that the intensity of the band edge emission peak slightly increases due to improvement of the crystallinity. On the other hand, the broad emission intensity considerably decreases due to removing crystal defect states. It is clearly shown that in X-ray characterization, the annealing processes not so strongly influence in the crystal formation, but in the PL characterization, that impact strongly to decrease the defect states which may influence in the photo-conduction characteristics.

### 3.2 Electrical and photo-electrical properties of ZnO thin film

The I-V characteristics were completely linear in the low voltage region, exhibiting the ohmic contact between the gold electrodes and the ZnO material as presented in Fig. 5. The resistivity (ρ) of the thin film with ZnO NRs could be calculated, referring to the electrode gap l = 0.2 mm and gap length w = 18.5mm as shows in Fig. 1(b). The thickness of sample is 700 nm, 676 nm and 505 nm of as-grown, annealed at 250 ºC and 450 ºC, respectively. The resistivity of the samples was decreased after the annealing process, due to reducing of the

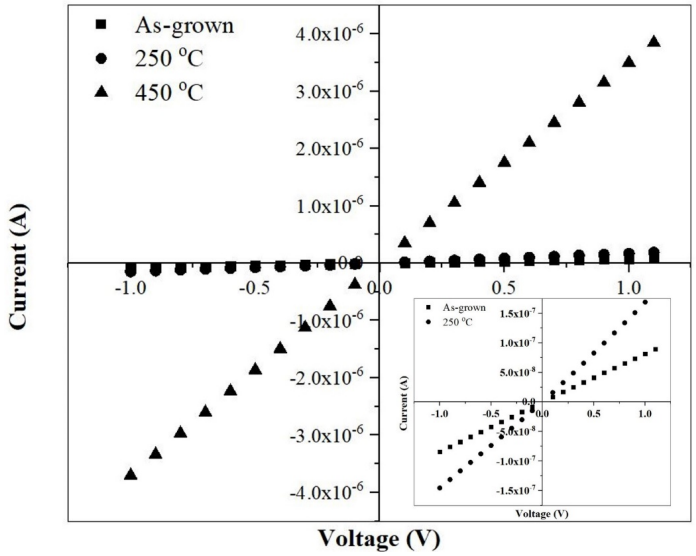


**Fig. 5.** I-V characteristic of ZnO thin films.

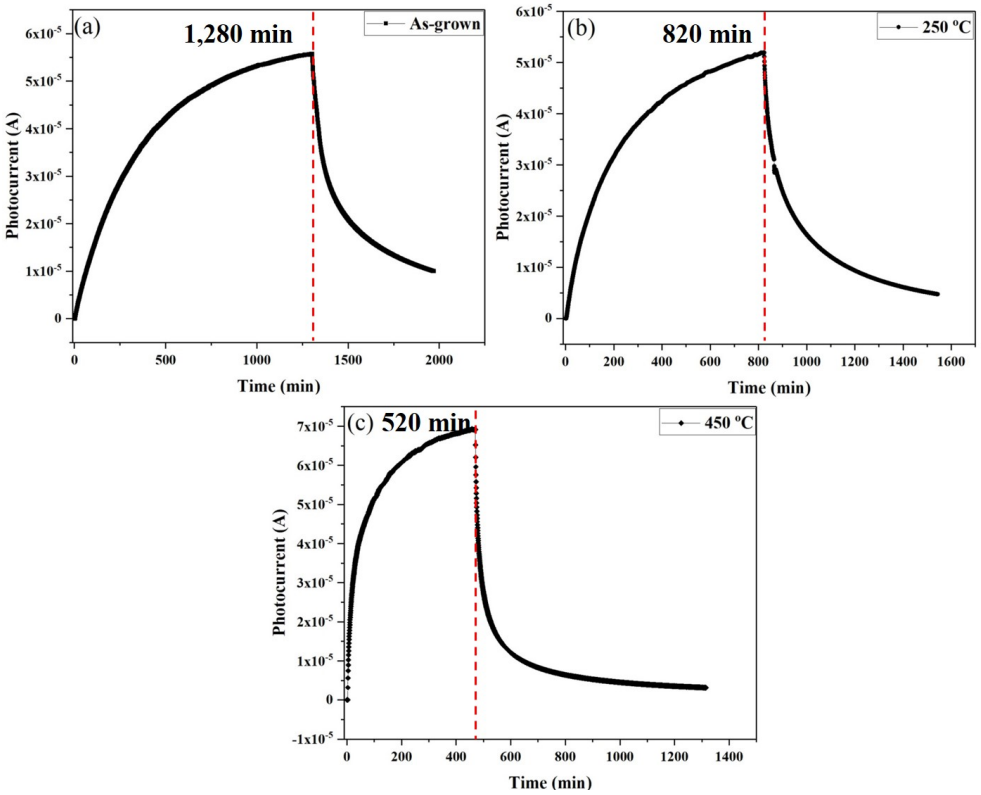


**Fig. 6.** The photocurrent characteristics of (a) as-grown, (b) annealed at 250 ºC, (c) annealed at 450 ºC.

defect concentration in ZnO NRs film [26]. The calculation resistivity values of ZnO NRs films are presented in Table 1.

The photocurrent properties of ZnO NRs thin film was carried under a bias voltage of 0.2 V in oxygen atmosphere as shown in Fig. 6 (a)-(c). All samples show a response to UV light in exponential- like pattern with different sensitivity. The ZnO NRs annealed at 450 ºC (Fig. 6(c)) shows highest response of photocurrent and fastest recovery to dark current comparing to annealing at 250 ºC and as-grown ZnO NRs (Fig. 6(b) and 6(a)), respectively. Moreover, the photocurrent of sample annealed at 450 ºC increases faster than other sample, according to PL results after annealed at high temperature the shallow defects on the structure of ZnO NRs reduced. The photo-excited moved directly to conduction band due to no obstructive with defect states in the structure.

After cutting off the UV light, the decay current is observed in accordance with the recombination process of the excited carriers and generally described as follows; [29]

$$\frac{dn(t)}{dt} = -Bp(t)n(t) = -Bn(t)^2 \tag{6}$$

where excited holes and electrons are supposed as same number. B is the recombination coefficient including time dependent and dispersive process in a random system. By introducing time-dependent part and dispersion parameter, the formulation is derived as followings [16][19][30];

$$B = Kt^{\beta-1} \tag{7}$$

$$\frac{dn}{dt} = -Kt^{\beta-1}n^2 \tag{8}$$

where β is called as the dispersion parameter (0<β<1). When t = 0, $n(0) = n_0$, the solution of equation (8) is as follows;

$$n(t) = n_0 \frac{1}{1+\left(\frac{n_0 Kt}{\beta}\right)^{\beta}} = n_0 \frac{1}{1+\left(\frac{t}{\tau}\right)^{\beta}} \tag{9}$$

where τ is an effective decay time in inhomogeneous media with dispersive nature.

$$\tau = \left(\frac{\beta}{n_0 K}\right)^{\frac{1}{\beta}} \tag{10}$$

As the photocurrent I(t) is proportional to n(t), the following decay current is derived as follows;

$$\frac{I(t)}{I_0} = \frac{1}{1+\left(\frac{t}{\tau}\right)^{\beta}} \tag{11}$$

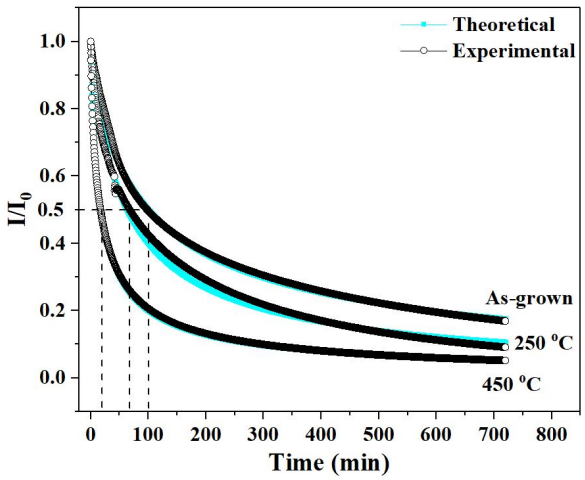


**Fig. 7.** The fitting of decay current between experiment and theoretical value calculated from equation (11).

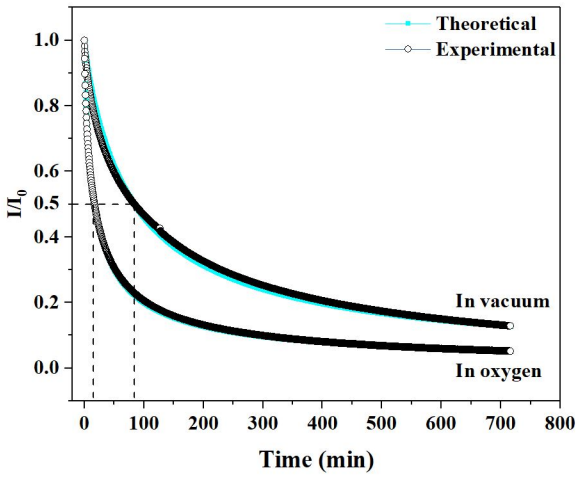


**Fig. 8.** The The fitting of decay current between experimental and theoretical value calculated from equation (11) in vacuum and oxygen atmosphere of sample annealed at 450 ºC.

where $I$ is the magnitude of the current, $I_0$ is the saturated photocurrent and $\tau$ is the effective decay time constant.

In figure 7, the experimental data were well fitted by the effective decay time constant ($\tau$) and dispersion parameter ($\beta$) using the equation (11). These recombination decay times and the dispersion parameter $\beta$ are presented in Table 1. The mechanism of photoconduction in these nanostructure and polycrystalline is not well understood, but in this paper, it is reasonable that the photoexcited carrier recombination arise in the inhomogeneous media.

Figure 8 shows the fitting decay current of ZnO NRs annealed at 450 ºC was observed, comparing to that in vacuum and oxygen atmosphere. In both cases, that shows the photo-response with the same tendency above derived equation (11). After cutting off the UV light,

the decay current was fitted by the equation (11) and obtained the effective decay time ($\tau_{ob}$) and the dispersion parameter ($\beta$). The ZnO NRs measured in oxygen atmosphere presented a very short decay time of 17 min comparing to 84 min in vacuum case.

$$\frac{1}{\tau_{ox}} = \frac{1}{\tau_{ob}} - \frac{1}{\tau_{v}} \tag{12}$$

where $\tau_{ob}$ is the obtained effective decay time, $\tau_v$ is vacuum ambient time constant and $\tau_{ox}$ is only oxygen assisted time constant [31]. Oxygen assisted recombination is a very dominant reaction in the oxygen environment and oxygen related decay time (14.14 min) is almost the same as the decay time observed in the oxygen ambient. However, oxygen reactions with the excited electrons and holes are now not clearly known and have to investigate more experimental studies in these photo-conductive experiments.

Therefore, it is shown that oxygen molecules strongly influenced on recombination process due to the oxygen molecules assisting the electron-hole recombination on the surface of ZnO NRs. The mechanism of the surface recombination with oxygen molecules is considered to occur by the two steps. Under UV radiation for long time, much electrons and holes are excited and stored near the conduction band and valence band as in equation (13). At the first, oxygen molecules collided on the nano-rods catch up electrons from the surface and result in super oxide molecules as shown in equation (14). The super oxide molecules will capture holes on the surface and returned to normal oxygen molecules as shown in equation (15). [12, 19, 31].

$$h\upsilon \rightarrow e^- + h^+ \tag{13}$$

$$O_2(g) + e^- \rightarrow O_2^- \tag{14}$$

$$h^+ + O_2^- \rightarrow O_2(g) \tag{15}$$

The interaction between electrons, holes and oxygen molecules on the surface of ZnO NRs represented as the catalytic reaction have to be more investigated on the activation energy from the temperature dependence of the decay characteristics and the difference for some kinds of molecules.

## 4. Conclusion

The vertically aligned ZnO NRs was prepared by the two steps; seeding by RF magnetron sputtering and nano-rods growth by low temperature hydrothermal method. Samples as-grown were annealed in air at 250 and 450 ºC and characterized on the crystallinity and the photo-electrical properties. The XRD patterns showed wurtzite crystal structure perfectly oriented along with the c-axis (0002) and vertically aligned to the substrate. The sample annealed at 450 ºC showed decreasing the defect states in the PL measurement and showed drastic decreasing electrical resistivity, and then photoconductive responses were strongly elevated. In these ZnO NRs thin films, photoconductive recombination process was shown as a bimolecular formulation and discussed for the reaction between electrons, holes and oxygen molecules. The oxygen molecules assisted surface recombination, and the photo-current decay was accelerated in the oxygen environment. The interaction kinetics of oxygen molecules on surface of ZnO NRs showing catalytic phenomenon are remained further investigation.

## Acknowledgement

Authors acknowledge Dr. K. Shimakawa, emeritus professor, Gifu University for guiding the formulation of photoconductivity in inhomogeneous media. The one (WS) of authors would like to express her gratitude to the Research Institute of Electronics, Shizuoka University to carry out the research work and financial support from Amano Fellowship.

## References

[1] Zhang Y. ZnO Nanostructure: Fabrication and Applications. Nanoscience and Nanotechnology: 1.1 Introduction of Nanomaterials. 2017;43:1–7.
[2] Bae SY, Choi HC, Na CW, Park J. Influence of incorporation on the electronic structure of nanowires Influence of In incorporation on the electronic structure of ZnO nanowires. Appl. Phys. Lett. 2005;86:033102.
[3] Kim KH, Park KC, Ma DY. Structural, electrical and optical properties of aluminum doped zinc oxide films prepared by radio frequency magnetron sputtering Structural, electrical and optical properties of aluminum doped zinc oxide. J. Appl. Phys. 2013;81: 7764.
[4] Hao X, Ma J, Zhang D, Yang T, Ma H. Thickness dependence of structural, optical and electrical properties of ZnO: Al films prepared on flexible substrates. Appl. Surf. Sci. 2001;183:137–142.
[5] Yang BP, Yan H, Mao S, Russo R, Johnson J, Saykally R, Morris N, Pham J, He R, Choi H. Controlled Growth of ZnO Nanowires and Their Optical Properties. Adv. Func. Mater. 2002;12:323–331.
[6] Jin BJ, Bae SH, Lee SY, Im S. Effects of native defects on optical and electrical properties of ZnO prepared by pulsed laser deposition. Matter. Sci. Eng. 2000;71:301-305.
[7] Dutta S, Chattopadhyay S, Sarkar A, Chakrabarti M, Sanyal D. Jana D., Progress in Materials Science Role of defects in tailoring structural , electrical and optical properties of ZnO. Prog. Mater. Sci. 2009;54:89-136.
[8] Basak D, Amin G, Mallik B, Paul GK, Sen SK, Photoconductive UV detectors on sol – gel-synthesized ZnO films. J. Cryst. Growth. 2003;256:73-77.
[9] Kushwaha A, Aslam M. Defect induced high photocurrent in solution grown vertically aligned ZnO nanowire array films. J. Appl. Phys. 2017;112:054316.
[10] Yi G, Wang C, Park WI. ZnO nanorods : synthesis , characterization and applications. Semicond. Sci. Technol. 2005;20:S22.
[11] Roqan I. High-Performance Ultraviolet-to-Infrared Broadband Perovskite Photodetectors Achieved via Inter-/Intraband Transitions. ACS Appl. Mater. Interfaces 2017;9(43):37832–37838.
[12] Soci C, Zhang A, Xiang B, Dayeh SA, Aplin DPR, Park J, Bao XY, Lo YH, Wang D. ZnO Nanowire UV Photodetectors with High Internal Gain. Nano Lett. 2007;7(4):1–7.
[13] Ahn M, Park K, Heo J, Park J, Kim D, Choi KJ, Lee J, Hong S. Gas sensing properties of defect-controlled ZnO-nanowire gas. Appl. Phys. Lett. 2008;93:263103.
[14] Tzeng SK, Hon MH, Leu IC. Persistent Photoconductivity of Solution-Grown ZnO–Based UV Detectors. J. Electrochem. Soc. 2011;158:H1188–H1193.
[15] Li S, Xu J, Shi S, Shi X, Wang X, Wang C, Zhang X, Liu Z, Li L. UV photoresponse properties of ZnO nanorods arrays deposited with CuSCN by SILAR method. Chem. Phys. Lett. 2015;620:50–55.

[16] Sakaguchi K, Shimakawa K, Hatanaka Y. Photoconductive Characteristics of Hydro-Oxygenated Amorphous Titanium Oxide Films Prepared by Remote Plasma-Enhanced Chemical Vapor Deposition. Jpn. J. Appl. Phyys. 2006;45:4183-4186.
[17] Mills A, Hunte SL. An overview of semiconductor photocatalysis. J. Photochem. Photobiol A Chemistry. 2000;108:1-35.
[18] Li QH, Gao T, Wang YG, Wang TH. Adsorption and desorption of oxygen probed from ZnO nanowire films by photocurrent measurements. Appl. Phys Lett. 2005;86:123117.
[19] Shimakawa K, Ganjoo A. AC photoconductivity of hydrogenated amorphous silicon : of long-range potential fluctuations. Phys. Rev. B. 2002;65:1-5.
[20] Biswas M, Mcglynn E, Henry MO, Mccann M, Rafferty A. Carbothermal reduction vapor phase transport growth of ZnO nanostructures : Effects of various carbon sources. J. Appl. Phys. 2009;105:094306.
[21] Chung R, Wang H, Li Y, Yeh P. Preparation and Sensor Application of Carbon Coated Zinc Oxide Nanorods Array. J. Aust. Ceram. Soc. 2013;49:81–88.
[22] Yan JT, Chen CH, Yen SF, Lee CT. Ultraviolet ZnO nanorod/P-GaN-heterostructured light-emitting diodes. IEEE Photonics Technol. Lett. 2010;22:146-148.
[23] Hejazi SMH, Majidi F, Tavandashti MP, Ranjbar M. The effect of heat treatment process on structure and properties of ZnO nano layer produced by solgel method. Mater. Sci. Semicond. Process. 2010;13:267–271.
[24] Narayanan GN, Ganesh RS, Karthigeyan A. Effect of annealing temperature on structural , optical and electrical properties of hydrothermal assisted Zinc Oxide Nano. Thin Solid Films. 2015;598:39–45.
[25] Wahid KA, Lee WY, Lee HW, The AS, Bien DSC, Azid IA. Effect of seed annealing temperature and growth duration on hydrothermal ZnO nanorod structures and their electrical characteristics. Appl. Surf. Sci. 2013;283:629-635.
[26] Sahdan MZ, Mamat MH, Salina M, Khusaimi Z, Noor UM, Rusop M. Heat treatment effects on the surface morphology and optical properties of ZnO nanostructures. Phys. Status Solidi. 2010;7:2286–2289.
[27] Hafiz M, Zuraida M, Musa K, Zahidi M, Rusop M. Performance of an Ultraviolet Photoconductive Sensor Using Well-Aligned Aluminium-Doped Zinc-Oxide Nanorod Arrays Annealed in an Air and Oxygen Environment, Jpn. J. Appl. Phys. 2011;50:6S.
[28] Zhang Y, Ma HL, Zhang Q, Peng J, Li J, Zhai M, Yu ZZ. Facile synthesis of well-dispersed graphene by γ-ray induced reduction of graphene oxide. J. Mater. Chem. 2012;22: 13064-13069.
[29] Rose AM. Human Right and Human Relation. RCA Review. 1951;12:362.
[30] Freitas RJ, Timor E, Shimakawa K, Republic C. Kinetics of the persistent photocurrent in a-Si:H. Int. J. Mod. Phys. A. 2016;30:1-7.
[31] Kittel C. Introduction to Solid State Physics. New York:J. Wiley and Sons, Inc.;1956. 366-367 p.